SEASONAL EFFECTS ON

WEST NILE VIRUS INFECTION

GUSTAVO CRUZ-PACHECO
IIMAS, UNAM
México, D.F. 04510
cruz@mym.iimas.unam.mx

LOURDES ESTEVA
Departamento de Matemáticas,
Facultad de Ciencias, UNAM,
México, D.F. 04510,
lesteva@servidor.unam.mx

CRISTOBAL VARGAS
Departamento de Control Automático,
CINVESTAV–IPN, A.P. 14–740,
México, D.F. 07000,
cvargas@ctrl.cinvestav.mx

Abstract

In this paper we analyze the impact of seasonal variations on the dynamics of WNV infection. We are interested in the generation of new epidemic peaks starting from an endemic state. In many cases, the oscillations generated by seasonality in the dynamics of the infection are too small to be observable. The interplay of this seasonality with the epidemic oscillations can generate new outbreaks starting from the endemic state through a mechanism of parametric resonance. As an example, we present the specific case of Fish Crow where we observed numerically this phenomenom.

Key-words: West Nile Virus - seasonality - parametric resonance - outbreak - oscillations

1 Introduction

West Nile Virus (WNV) fever is a vector borne disease. Birds are the natural reservoir of this virus, and humans, horses and probably other vertebrates are circumstantial hosts; that is, they can be infected but they do not transmit the disease. Then, WNV is maintained in nature in a mosquito-bird-mosquito-transmission cycle (Campbell et al, 2002; Hayes, 1989). The disease has been endemic in countries of Africa, Western Asia and Europe for decades (Hayes, 1989). The virus was detected for the first time in North America in 1999, during an outbreak in New York City (CDC, 1999). It rapidly spread across the USA causing great mortality in humans, horses and birds.

Data of WNV in the United States reveals clearly an epidemic front moving from east to west. The annual maximal prevalence of the disease occurs between late July and early September. In the states where the disease appeared in 1999, it is observed a decline of the maximal prevalence, which reveals that the disease is evolving toward an endemic situation where the infected proportion is rather small (CDC, 2005). It is very important to understand how new large epidemic peaks could be generated from this endemic situation.

As many arbovirus diseases, WNV fever is characterized by long intervals where little or no evidence of its existence can be detected. At apparently erratic intervals, there is a sudden recrudescence developing into large outbreaks. Studies of such epidemics often suggest by association that weather-

related factors could have been responsible for this recrudescence. There have been many speculative explanations about this association, but the timing of recrudescence still remains without a satisfactory explanation (Reiter, 2001).

Seasonality impacts the biology of mosquitoes in different forms: changes in reproduction, population size and blood feeding, have been recorded in literature. For example, in South Florida, the proportion of blood meals taken by *Cx. nigripalpus* from birds is higher during winter than in summer, independently of the bird population size (Edman and Taylor, 1974).

We consider that seasonal variations of the mosquito population and the host population interact in such a way that give rise to periodic outbreaks of vector borne diseases. It is important to notice that there are two different mechanisms responsible of the epidemic oscillations, namely, one extrinsic associated to the seasonal changes, and the other intrinsic associated to the dynamic interaction between host and vector populations. There is no agreement about which of the two refereed mechanisms may have more influence on the recrudescence of the disease. Some studies point to seasonal oscillations as the more relevant factor for the periodicity and severity of the outbreaks (Lord and Day, 2001). In contrast, based on a retrospective analysis of time series of epidemiological and meteorological data for Dengue in Bangkok, Hay et al. (2000) concluded that intrinsic population dynamics is the more plausible explanation for the observed interepidemic periods. Their conclusion is based on the fact that the periodicity of the disease (three years) is different that the periodicity associated with the seasonal changes (one year).

In this work we study the impact of seasonal variations of the mosquito population on the dynamics of WNV. It is a continuation of a previous work (Cruz et al., 2005) where we modeled bird-mosquito transmission cycle, assuming that mosquito population size remains constant. Here, we assumed that this population changes annually. For some values of the intrinsic frequency, corresponding to data collected for one species of bird, we found a kind of resonance known as *parametric resonance* (Landau and Lifschitz, 1960; Magnus and Winkler, 1966), which is characterized by exponential growth of the amplitude of the oscillations. We shall dwell on this concept posteriorly in the text.

We propose the existence of a synergism between the intrinsic and extrinsic mechanisms that results in large observable epidemic peaks with a period not necessarily equal to one year. This synergism is a consequence of resonant effects between the natural frequency of the disease, resulting

from the intrinsic vector-host dynamics, and the external seasonal frequency. It is believed that the size of the increment on the number of mosquitoes is the most important factor (Lord and Day, 2001) for recrudescence of the disease. However, we found that resonance phenomena are responsible for larger epidemic peaks.

2 The basic model

The following system of nonlinear differential equations was proposed in (Cruz et al., 2005) to explore the temporal mosquito-bird cycle transmission of WNV with constant mosquito population. The system consists of the interactions among susceptible and infective individuals of the two species, assuming that the transmission of the disease is only by mosquito bites and vertical transmission in the vector population,

$$\begin{aligned}
\frac{dS_a}{dt} &= \Lambda_a - \frac{b\beta_a}{N_a} I_v S_a - \mu_a S_a \\
\frac{dI_a}{dt} &= \frac{b\beta_a}{N_a} I_v S_a - (\gamma_a + \mu_a + \alpha_a) I_a \\
\frac{dR_a}{dt} &= \gamma_a I_a - \mu_a R_a \\
\frac{dS_v}{dt} &= \mu_v S_v + (1-p)\mu_v I_v - \frac{b\beta_v}{N_a} I_a S_v - \mu_v S_v \\
\frac{dI_v}{dt} &= p\mu_v I_v + \frac{b\beta_v}{N_a} I_a S_v - \mu_v I_v \\
\frac{dN_a}{dt} &= \Lambda_a - \mu_a N_a - \alpha_a I_a,
\end{aligned} \tag{2.1}$$

where S_a, I_a, R_a denote the number of susceptibles, infective and recovered in the avian population, $N_a = S_a + I_a + R_a$ the total bird population; S_v, I_v the number of susceptible and infective in the vector population, and $N_v = S_v + I_v$ the total number of mosquitoes.

The parameters in the model are the recruitment rate Λ_a, and the natural mortality rate μ_a of the bird population; the mortality rate of mosquitoes μ_v; the biting rate of mosquitoes b; β_a and β_v the transmission probabilities, γ_a the recovery rate, and α_a the disease related death in the avian population, and finally p is the proportion of infected offsprings from an infected

mosquito.

In order to reduce the number of parameters and simplify system (2.1), the bird and vector population are normalized

$$s_a = \frac{S_a}{\Lambda/\mu_a}, \quad i_a = \frac{I_a}{\Lambda/\mu_a}, \quad r_a = \frac{R_a}{\Lambda/\mu_a}, n_a = \frac{N_a}{\Lambda/\mu_a}, \quad s_v = \frac{S_v}{N_v}, \quad i_v = \frac{I_v}{N_v}.$$

Since $r_a = n_a - s_a - i_a$ and $s_v = 1 - i_v$, the equations for r_a and s_v are omitted. Then, system (2.1) is equivalent to the following system for the proportions:

$$\begin{aligned} \frac{ds_a}{dt} &= \mu_a - \frac{b\beta_a m}{n_a} i_v s_a - \mu_a s_a \\ \frac{di_a}{dt} &= \frac{b\beta_a m}{n_a} i_v s_a - (\gamma_a + \mu_a + \alpha_a) i_a \\ \frac{di_v}{dt} &= \frac{b\beta_v}{n_a} i_a (1 - i_v) - (1-p)\mu_v i_v \\ \frac{dn_a}{dt} &= \mu_a - \mu_a n_a - \alpha_a i_a, \end{aligned} \tag{2.2}$$

in the subset $\Omega = \{0 \leq s_a, 0 \leq i_a, s_a + i_a \leq n_a \leq 1, 0 \leq i_v \leq 1\}$. Here $m = \dfrac{N_v}{\Lambda_a/\mu_a}$, is the ratio between the vector population and the disease-free equilibrium bird population value.

The basic reproductive number of the disease is

$$R_0 = \sqrt{\frac{mb^2\beta_a\beta_v}{(\gamma_a + \mu_a + \alpha_a)(1-p)\mu_v}}. \tag{2.3}$$

If R_0 is less than one, the disease will fade out, since an infective individual will be replaced with less than one new case. On the other hand, if R_0 is greater than one, the mosquito and bird populations will approach an

endemic steady state $P_1 = (\hat{s}_a, \hat{i}_a, \hat{i}_v, \hat{n}_a)$, given by the following relations

$$\begin{aligned} \hat{s}_a &= \frac{\mu_a - (\gamma_a + \mu_a + \alpha_a)\hat{i}_a}{\mu_a} \\ \hat{n}_a &= \frac{\mu_a - \alpha_a \hat{i}_a}{\mu_a} \\ \hat{i}_v &= \frac{\mu_a b \beta_v \hat{i}_a}{(b\beta_v\mu_a - \alpha_a(1-p)\mu_v)\hat{i}_a + (1-p)\mu_v\mu_a}, \end{aligned} \tag{2.4}$$

where $\hat{i}_a$ is the unique root of the equation

$$r(i_a) = Ai_a^2 + Bi_a + C \tag{2.5}$$

with

$$\begin{aligned} A &= [b\beta_v\mu_a - \alpha_a(1-p)\mu_v]\frac{\alpha_a}{\mu_a}, \\ B &= 2\alpha_a(1-p)\mu_v - b\beta_v\mu_a - (1-p)\mu_v(\gamma_a + \mu_a + \alpha_a)R_0, \\ C &= \mu_a(1-p)\mu_v(R_0 - 1), \end{aligned}$$

in the interval $\hat{i}_a \in (0, \dfrac{\mu_a}{\mu_a + \gamma_a + \alpha_a})$.

Figure 1 illustrates the typical behavior of the proportion of infective birds. We notice that this proportion approaches the endemic equilibrium through damped oscillations. The parameter μ_a is in general several orders of magnitude smaller than the other parameters of the model (see Table 1), since the life span of birds is in general larger than one year, whereas the length of the infected period is a few days. Then under this situation there exist damped oscillations for $R_0 > 1$.

FIGURE 1

Proposition. *Assume $R_0 > 1$ and $\mu_a << 1$, then the solutions of system (2.2) oscillate to the endemic equilibrium*

Proof. The existence of oscillations depends on whether the characteristic eigenvalues around the equilibrium P_1 have nonzero imaginary part. Such eigenvalues are μ_a and the roots of the polynomial

$$\lambda^3 + P\lambda^2 + Q\lambda + R, \tag{2.6}$$

where the coefficients

$$\begin{aligned} P &= \frac{\mu_a}{\hat{s}_a} + \frac{mb\beta_a\hat{i}_v\hat{s}_a}{\hat{i}_a\hat{n}_a} + \frac{b\beta_v\hat{i}_a}{\hat{i}_v\hat{n}_a} \\ Q &= \frac{\mu_a b\beta_v\hat{i}_a}{\hat{s}_a\hat{i}_v\hat{n}_a} + \frac{mb^2\beta_a\beta_v\hat{s}_a\hat{i}_v}{\hat{n}_a^2} + \frac{mb\beta_a i_v(\mu_a\hat{n}_a - \alpha_a\hat{i}_a\hat{s}_a)}{i_a n_a^2} \\ R &= \frac{\mu_a mb^2\beta_a\beta_v((\hat{n}_a - \hat{s}_a) + \hat{s}_a\hat{i}_v)}{\hat{n}_a^3} - \frac{\alpha_a mb^2\beta_a\beta_v\hat{s}_a\hat{i}_a}{\hat{n}_a^3} \end{aligned} \tag{2.7}$$

are all positive. Substituting in (2.7) the expressions for $\hat{s}_a$, $\hat{i}_a$, $\hat{i}_v$ and $\hat{n}_a$ given in (2.4), it can be seen that $P \approx 1$, $Q \approx \mu_a$ and $R \approx \mu_a$. Then, up to μ_a^2, the roots of (2.6) have the form

$$\begin{aligned} \lambda_0 &= -P + O(\mu_a), \\ \lambda_{1,2} &= -\frac{Q}{2P} \pm i\sqrt{\frac{R}{P}} + O(\mu_a^2), \end{aligned} \tag{2.8}$$

which implies that the solutions of (2.2) will oscillate toward the endemic equilibrium with frequency approximately given by $\sqrt{\frac{R}{P}}$. This proves the proposition.

We call the imaginary part of the eigenvalues of (2.6) the *natural frequency* of system (2.2).

The numerical solutions of (2.2) showed that the maximal prevalence in the avian population is very high when the disease is introduced for the first time. In the cases analyzed, between two and four tenths of the avian population got infected during the first epidemic peak. This first outbreak fades out after around 30 days followed by a period of time where the infection seems to disappear. After this period, a second epidemic peak appears, and the longer it takes to appear the higher it is. This is explained by the fact that when the period between the first two peaks is large, more susceptible birds are recruited by the end of this period, and their number becomes close to the initial data. Thus, the situation is more alike to the one of the initial conditions. After the second peak, the infected population size will approach the endemic prevalence value through damped oscillations. In the observed

cases, even when the first outbreak is very high, the endemic prevalence is not (it is less than 0.05 percent of the total population size), see Figure 1. It is important to remark that only the first two peaks have a size relevant from an epidemiological point of view, the rest of the oscillations are too small to be distinguished from the endemic value.

The above behavior was explained in terms of R_0. If $R_0^2 s_a s_v > 1$ then s_a and s_v decrease and the infectious proportions i_a and i_v first increase to a peak and then decrease because there are not sufficient susceptible to be infected and a part of the infected ones get recovered or die. When the susceptible fractions get large enough due to recruitment of new susceptible, there are secondary smaller epidemics, and thus the solution oscillate to the endemic equilibrium.

3 Seasonal variations

Almost all species of arthropods present seasonal variations on their activity, and there is a wide variety of seasonal arrangements of active and dormant phases in their life cycles (Reiter, 2001). Thus, *Aedes* mosquitoes survive winter season in the egg stage, whereas *Culex* and *Anopheles* survive as adults. Weather variations are determinant in the abundance of mosquitoes due to the availability of food or breeding sites, which implies that seasonality is different for different species.

In this section we assume that the mosquito population, $N_v(t)$, follows a periodic pattern of period T which depends on its species. In particular, we shall assume that $N_v(t)$ is given by

$$N_v = \bar{N}_v - A_v \cos(\omega t), \tag{3.9}$$

where $\bar{N}_v$ is the mean mosquito population size. The amplitude and frequency of the variation of the mosquito population are given by $2A_v$ and ω, respectively.

In this manner, (2.2) becomes the following non-autonomous system

$$\begin{aligned}
\frac{ds_a}{dt} &= \mu_a - \frac{b\beta_a(\bar{n}_v - a_v\cos(\omega t))}{n_a} i_v s_a - \mu_a s_a \\
\frac{di_a}{dt} &= \frac{b\beta_a(\bar{n}_v - a_v\cos(\omega t))}{n_a} i_v s_a - (\gamma_a + \mu_a + \alpha_a) i_a \\
\frac{di_v}{dt} &= \frac{b\beta_v}{n_a} i_a(1 - i_v) - \frac{a_v\omega\sin(\omega t)}{\bar{n}_v - a_v\cos(\omega t)} i_v - (1-p)\mu_v i_v \qquad (3.10) \\
\frac{dn_a}{dt} &= \mu_a - \mu_a n_a - \alpha_a i_a,
\end{aligned}$$

where $\bar{n}_v = \dfrac{\bar{N}_v}{\Lambda/\mu_a}$, and $a_v = \dfrac{A_v}{\Lambda_a/\mu_a}$.

In the sequel we analyze numerically system (3.10). For the simulations presented here we used the values $\omega = \dfrac{2\pi}{356} = 0.0172$ day^{-1}, $\bar{n}_v = 5$ and $a_v = 3$. The rest of the parameter values are retained from Cruz et al, 2005; Komar et al, 2003; Oliver Jr., 1961a,b; The University of Michigan Museum of Zoology, 2004, and they are shown in Table 1. In all cases $\beta_a = 1$, $\mu_v = 0.06$ day^{-1}. The natural frequency corresponds to the imaginary part of the eigenvalues given in (2.8).

TABLE 1

In six of the eight species of birds, we observed that the epidemic peaks follow passively the periodic oscillations of the vector population, and probably this is the most likely scenario in nature. The amplitude of the oscillations was small, which implies that in many cases the epidemic peaks are not observable. On the other hand, for the parameter values corresponding to Fish Crow and Ring-billed Gull, the observed oscillations present the typical behavior of the so called parametric resonance.

Parametric resonance appears when in an oscillatory system one of its parameters starts to oscillate by itself. This kind of resonance comes from inside the system as oppose to the classical resonance which originates from external excitations. The canonical example of parametric resonance is the swing, where a child can start to swing by himself from rest by moving his legs, and therefore changing periodically the center of mass of the system. Two properties characterize this kind of resonance: the exponential growth

of the amplitude of the oscillations, and the fact that the domains of resonant frequencies are whole intervals. In classical resonance the amplitude increases linearly or at most as a polynomial, and the resonance frequencies are isolated points (Magnus and Winkler, 1966).

Returning to the examples of Fish Crow and Ring-billed Gull, we found that the epidemic peaks not just follow passively the periodic oscillations of the vector population, but react actively to the periodic disturbance. As a result, the amplitude of the oscillation of the infected proportion initially grows exponentially due to the parametric resonance. When this amplitude is sufficiently large the nonlinear terms become important, slowing down the growth, and the system goes to a state of bounded oscillations as can be seen in Figure 2 for the case of Fisch Crow.

FIGURE 2

In Figure 2 we compare the resonant and non-resonant cases. Using data of Fish Crow and Common Grackle we solved system (3.10) starting from the endemic states. The resonant case is illustrated by the temporal course of the infected proportion of Fish Crow. For this species, the natural frequency ($\omega_n = 0.011$ days^{-1}) and the annual frequency ω satisfy $3\omega_n = 2\omega$ up to the third decimal place, which implies that they are resonant. As can be seen in the figure, new infection peaks develop with size larger than the secondary infection peak of Figure 1, where constant vector population was assumed. These new peaks grow rapidly as a result of the resonance, but saturate to a bounded state due to the nonlinear effects. Notice that even when the seasonal oscillations are annual, the infection peaks have period close to two years. This is a common feature of parametric resonance (Hale, 1969). Therefore, annual seasonal oscillations do not necessarily produce annual outbreaks.

The temporal course of Common Grackle infected proportion corresponds to the non-resonant case. The natural frequency ($\omega_n = 0.014$ days^{-1}) of this species is not resonant with the annual frequency. As can be seen in the figure, the infected proportion follows the seasonal oscillations of the vector population with the same annual period, and the amplitude of the oscillations

do not grow.

FIGURES 3a AND 3b

In Figure 3 we observe the temporal course of the infected bird proportion under a sudden change of the ratio m, between vector and host population at time $t = 4000$. For $t \leq 4000$, m is constant and equal to five. In Figure 3a, m jumps from 5 to 8, meanwhile in Figure 3b, $m(t) = 5 - 3\cos\left(\frac{2\pi t}{365}\right)$ for $t \geq 4000$, with $m(4000) \approx 3.918$ In the first case the average number of mosquitoes is bigger, but its effect on the disease is weaker, since there is only a small epidemic peak and immediately the infection fraction returns through damped oscillations to virtually the previous endemic prevalence. This illustrates that in the resonant case, the frequency of oscillations on the number of mosquitoes has a more important effect on the recrudescence of the disease than the total increment of such population.

FIGURES 4a AND 4b

These outbreaks can also be explained in terms of the basic reproductive number R_0, given by (2.3). As we know, a necessary condition for an outbreak is $R_0^2 s_a s_v > 1$, where s_a and s_v denote the fractions of susceptible birds and mosquitoes. In the presence of seasonal changes of the vector population, R_0 is a periodic function with the same period as $N_v(t)$. The maximal epidemic peaks develop when $R_0^2 s_a s_v$ reaches its maximum value which is bigger than one (Figures 4a and 4b). These results show the interplay between the external frequency of the oscillations of R_0 due to seasonality, and the natural frequency of the epidemic imposed by the recruitment of susceptibles birds and mosquitoes, which gives the oscillations observed in Figure 4a.

FIGURE 5

4 Conclusions

In this paper we formulated a model to study the influence of seasonal variations of mosquito population on the transmission of WNV disease. This is a continuation of our previous work in which vector population was considered constant. Here, we used the data of eight species of birds to investigate nu-

merically the relation between the intrinsic interepidemic period (depending on the epidemic and demographic parameters of host and vectors), and the extrinsic periodic oscillations of the vector population imposed by seasonality.

We found numerically that for six species, the infected proportion only follows passively the seasonal variations, with the size of the oscillations very small and therefore not observable. On the other hand, for Fish Crow and Ring-billed Gull we obtained that the interaction between the intrinsic and extrinsic oscillations is responsible for the origin of large epidemic peaks, through a mechanism of parametric resonance.

It is clear that the development, behavior and survival of mosquitoes, as well as the transmission of the disease are strongly influenced by climatic factors. In some places, the end of summer is the time of the year where the mosquito population increases notably, and it is expected that a jump in the vector population size will produce an increment of the transmission of the disease. Nevertheless, for an endemic situation, this increment could be negligible, as can be seen in Figure 3a, where only a small epidemic peak is observed followed by damped oscillations approaching the endemic equilibrium.

The model indicates that for arbovirus infections, a sudden recrudescence from an endemic situation could have its origin in the interplay between intrinsic and extrinsic oscillations, and it is not just a simple consequence of the vector population growth associated to climatic changes, such as "el Niño" or global warming. This situation was clearly founded for the Fish Crow species where the interplay gives large epidemic peaks every two years. This also shows that seasonality not necessarily produces annual peaks, as could be thought, but the frequency of the new outbreaks depends on the relationship between the intrinsic and seasonal frequencies.

In this paper we posed the question of how seasonal changes can generate new outbreaks beginning at endemic states. Even for a simplified model as (3.10), the long time dynamics is rather complex as can be seen in Figure 5. There, it can be observed that up to time $t = 20000$, the oscillations do not approach a state of constant amplitude. We believed that this should be a subject of further study.

Acknowledgments. G.C.P. is grateful to Ana Cecilia Pérez for technical support. He was supported by Grant U47899-F from CONACYT.

References

[1] Campbell, L. G., Martin, A. A., Lanciotti, R. S., Gubler, D. J., 2002. West Nile Virus. The Lancet Infect. Dis. 2, 519-529.

[2] Center for Disease Control and Prevention (CDC), 1999. Update: West Nile-like viral encephalitis-New York, 1999. Morb Mortal Wkly. Rep. 48, 890-892.

[3] Center for Disease Control and Prevention (CDC), 2005. *www.westnilemaps.usgs.gov/.*

[4] Cruz-Pacheco, G, Esteva, L., Montaño-Hirose, J. A., Vargas, C., 2005. Modelling the dynamics of West Nile Virus. Bull. Math. Biol. 67, 1157-1172.

[5] Edman, J. D., Taylor, D. J., 1974. Host-feeding patterns of Florida mosquitoes. III. *Culex (Culex)* and *Culex (Neoculex).* J. Med. Entomol. 11, 95-104.

[6] Hale, J.K., 1969. Ordinary Differential Equations. Krieger Publishing, Florida.

[7] Hay, S. I., Myers, M. F., Burke, D. S., Vaughn, D. W. et al., 2000. Etiology of interepidemic periods of mosquito-borne disease. Proc. Natl. Acad. Sci. USA. 97, 9335-9339.

[8] Hayes C. G., 1989. West Nile fever . In: Monath, T. P. (Ed.), The arboviruses: Epidemiology and ecology, Vol. V. CRC Press, Florida, pp. 59-88.

[9] Komar, N., Langevin, S., Hinten, S., Nemeth, N., Edwards, E., *et al.*, 2003. Experimental Infection of North American Birds with the New York 1999 Strain of West Nile Virus. Emerg. Infect. Dis. 9 (3), 311-322.

[10] Landau, L. D., Lifschitz, E. M., 1960. Mechanics. Pergamon Press, Oxford.

[11] Lord, C. C., Day, F. J., 2001. Simulations studies of St. Louis Encephalitis and West Nile Viruses: The impact of bird mortality. Vector Borne and Zoonotic Diseases. 1, 317-329.

[12] Magnus, W., Winkler, S., 1966. Hill's Equation. Dover, New York.

[13] Oliver Jr., L. A., 1961a. Crows and Jays-Corvidae. In: Birds of the World. Golden Press, New York.

[14] Oliver Jr., L. A., 1961b. Gulls and Terns-Laridae. In: Birds of the World. Golden Press, New York.

[15] Reiter, P., 2001. Climate change and mosquito-borne disease. Environmental Health Perspectives Suplements. 109, 141-161.

[16] The University of Michigan Museum of Zoology, 2004. Animal Diversity Web. http://www.animaldiversity.ummz.umich.edu

Common name	β_v	γ_a day^{-1}	α_a day^{-1}	μ_a day^{-1}	$\tilde{R}_0$	ω_n day^{-1}
Blue Jay	0.68	0.26	0.15	0.0002	5.89	0.0267
Common Grackle	0.68	0.33	0.07	0.0001	5.97	0.01496
House Finch	0.32	0.18	0.14	0.0003	4.57	0.02733
American Crow	0.5	0.31	0.19	0.0002	4.58	0.02109
House Sparrow	0.53	0.33	0.1	0.0002	5.08	0.01898
Ring-billed Gull	0.28	0.22	0.1	0.0003	4.28	0.02087
Black-billed Magpie	0.36	0.33	0.16	0.0001	3.92	0.01590
Fish Crow	0.26	0.36	0.06	0.0002	3.60	0.011150

Table 1. Epidemiological and demographic parameters of model (3.10).

FIGURE CAPTIONS

Figure 1. Temporal course of the proportion of infected birds obtained with model (2.2). The parameters are given in Table 1 for Fish Crow, and the initial conditions are $s_a = 1, i_a = 0, i_v = 0.001, n_a = 1$.

Figure 2. Numerical solutions of system (3.10) for Common Grackle and Fish Crow starting from their endemic equilibrium. The extrinsic frequency is $\omega = \frac{2\pi}{365}$ days^{-1}, and the other parameters are given in Table 1.

Figure 3. Temporal course of the infected bird population under a sudden change of the ratio m between vector and host population at time $t = 4000$. a) m changes from $m = 5$ to $m = 8$. b) m changes from $m = 5$ to $m(t) = 5 - 3cos(\frac{2\pi t}{365})$ for $t \geq 4000$.

Figure 4. a) Temporal course of the infected Fish Crow population starting from their endemic state. b) Temporal course of $R_0(t)s_a(t)s_v(t)$ for Fish Crow. The parameters in both figures are the same as in Figure 2.

Figure 5. Long time behavior of the infected proportion of Fish Crow with data as in Figure 2.

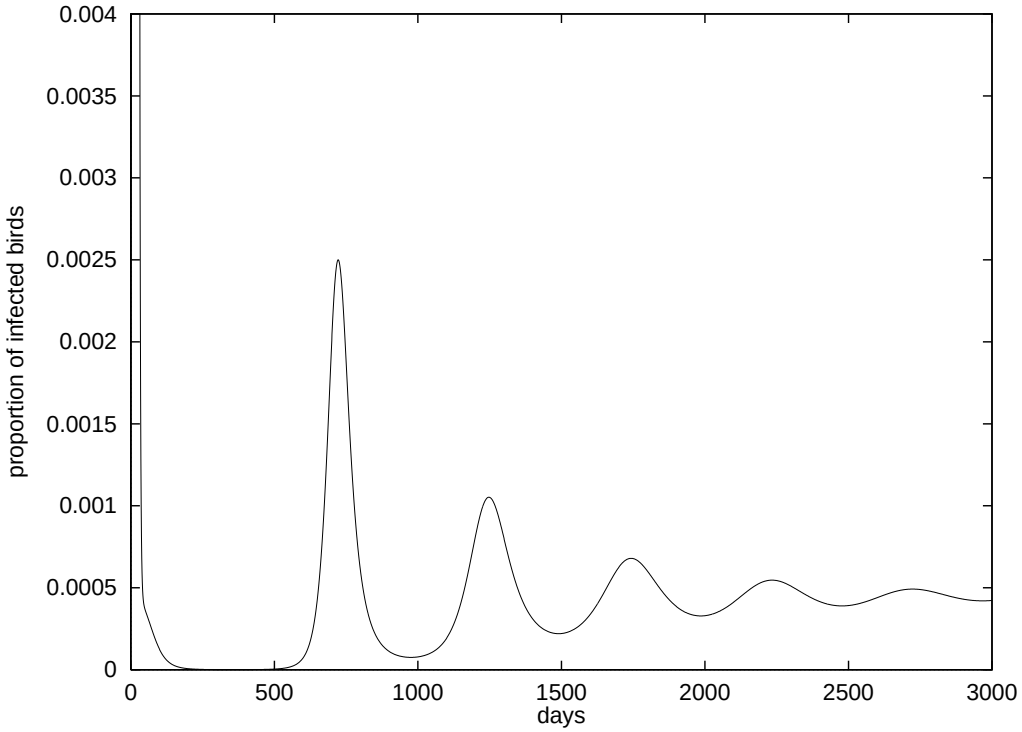
0.004
0.0035
0.003
0.0025
0.002
0.0015
0.001
0.0005
0
proportion of infected birds
0
500
1000
1500
2000
2500
3000
days

Figure 1:

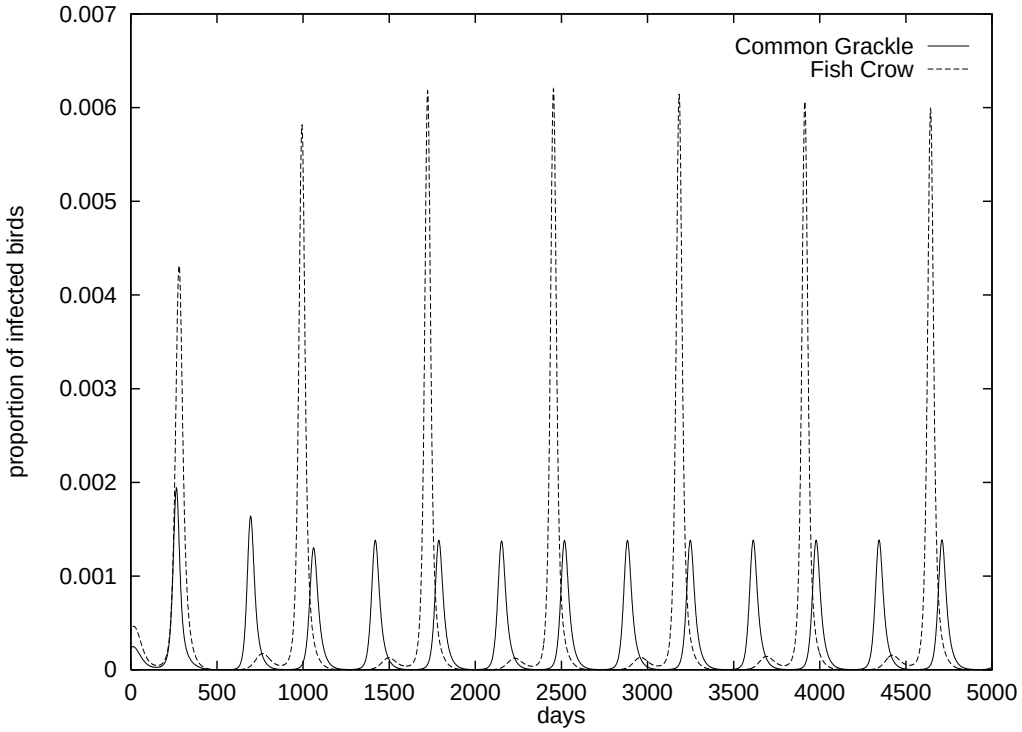
0.007
0.006
0.005
0.004
0.003
0.002
0.001
0
proportion of infected birds
0
500
1000
1500
2000
2500
3000
3500
4000
4500
5000
days
Common Grackle
Fish Crow

Figure 2:

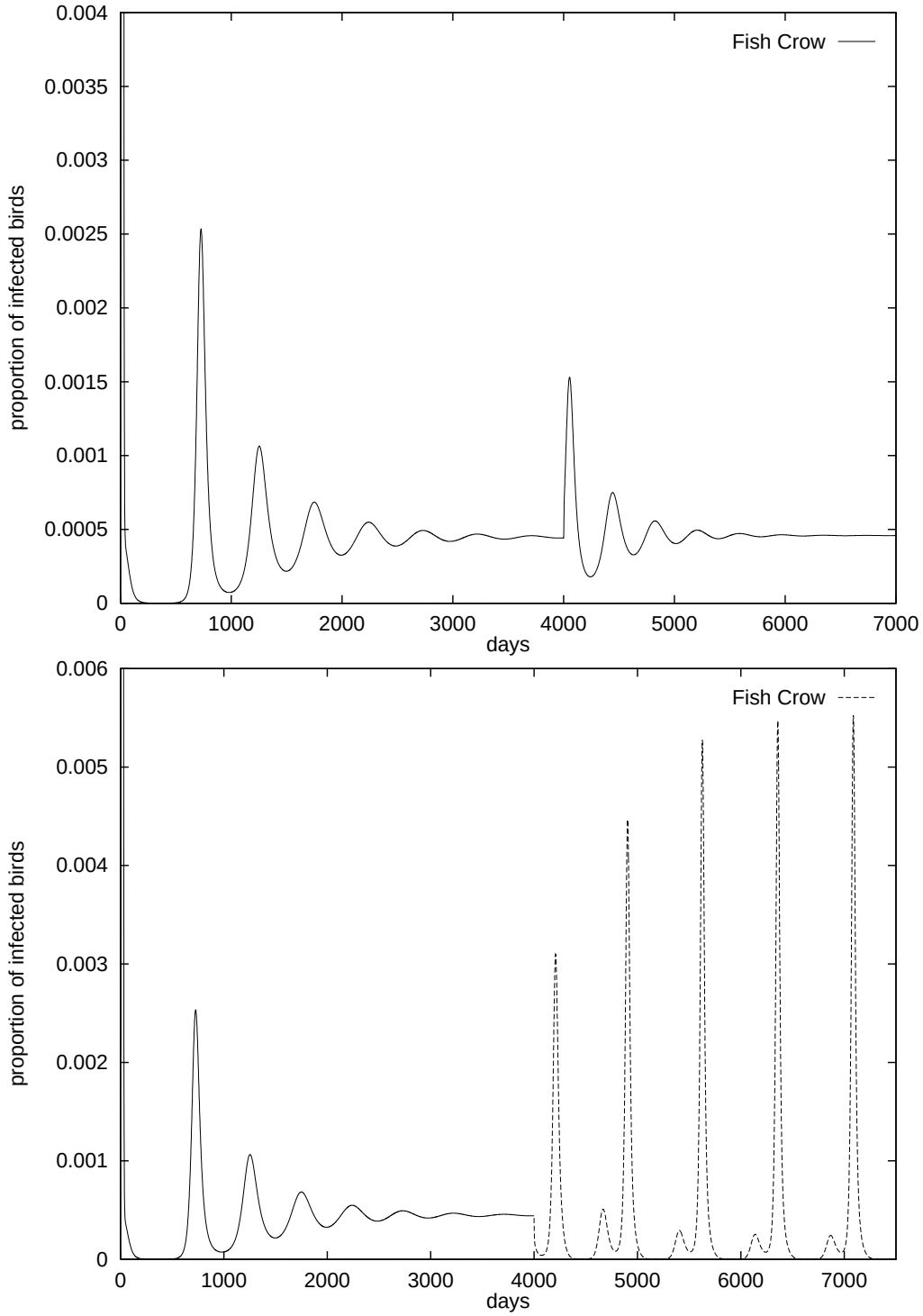
0.004
0.0035
0.003
0.0025
0.002
0.0015
0.001
0.0005
0
proportion of infected birds
Fish Crow
0
1000
2000
3000
4000
5000
6000
7000
days
0.006
0.005
0.004
0.003
0.002
0.001
0
proportion of infected birds
Fish Crow
0
1000
2000
3000
4000
5000
6000
7000
days

Figure 3:

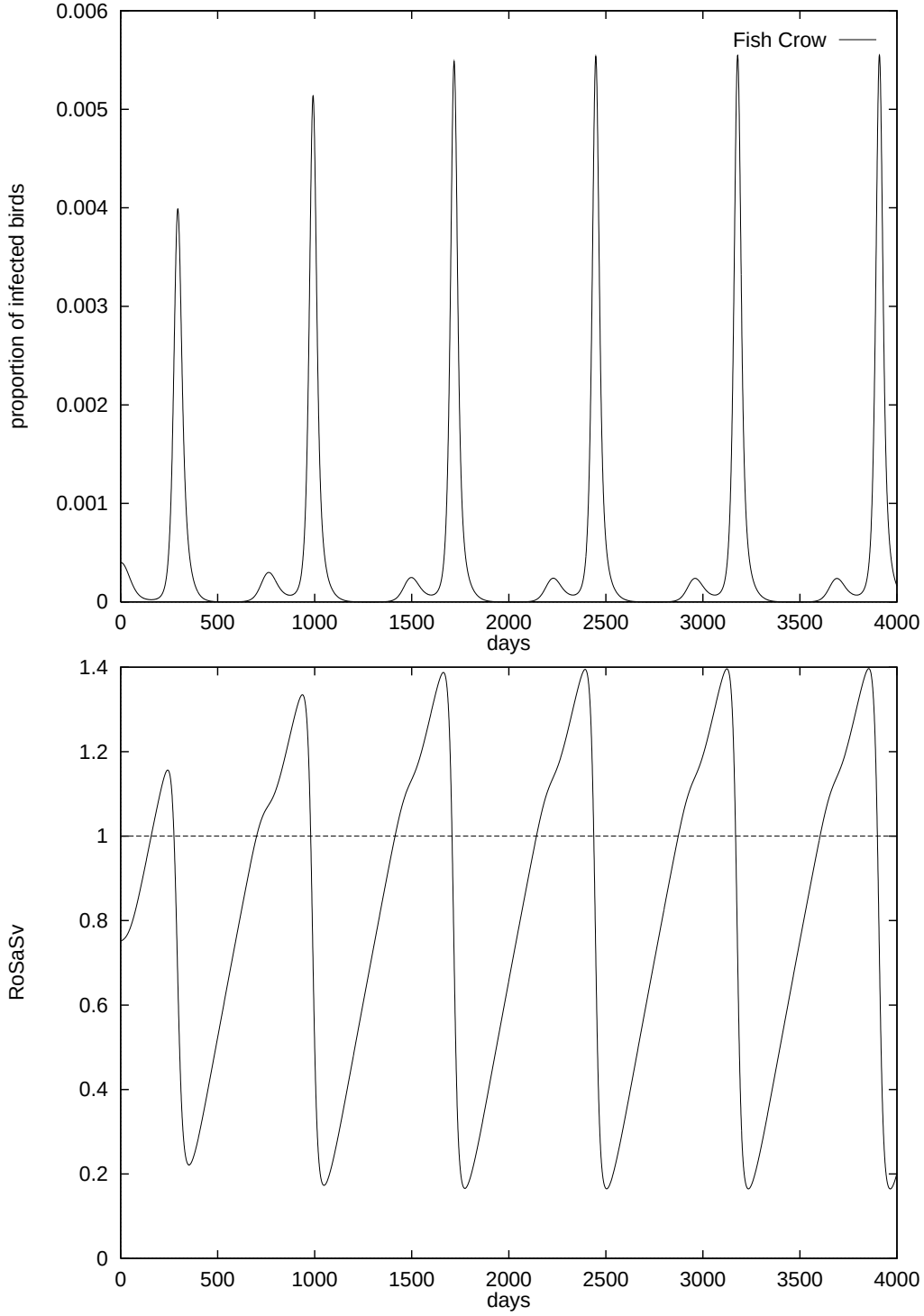
Fish Crow
proportion of infected birds
0.006
0.005
0.004
0.003
0.002
0.001
0
0
500
1000
1500
2000
2500
3000
3500
4000
days
RoSaSv
1.4
1.2
1
0.8
0.6
0.4
0.2
0
0
500
1000
1500
2000
2500
3000
3500
4000
days

Figure 4:

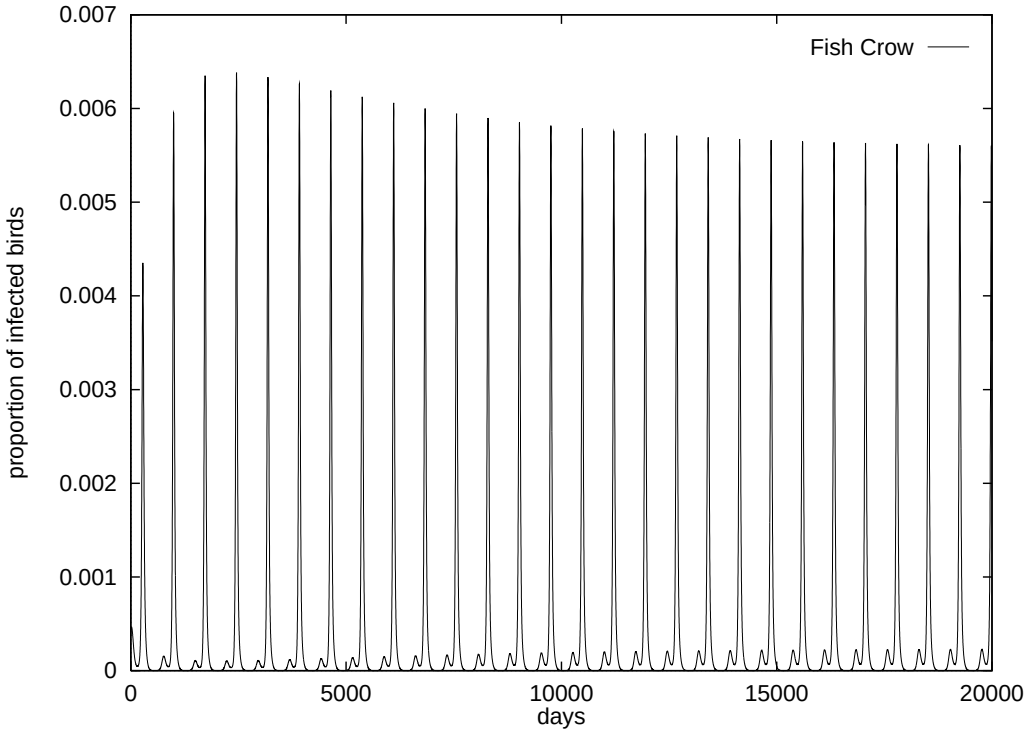
0.007
0.006
0.005
0.004
0.003
0.002
0.001
0
proportion of infected birds
0
5000
10000
15000
20000
days
Fish Crow

Figure 5: